Chem Catalysis

CellPress

Article

Visible-light-induced catalytic construction of tricyclic aza-arenes from halopyridines

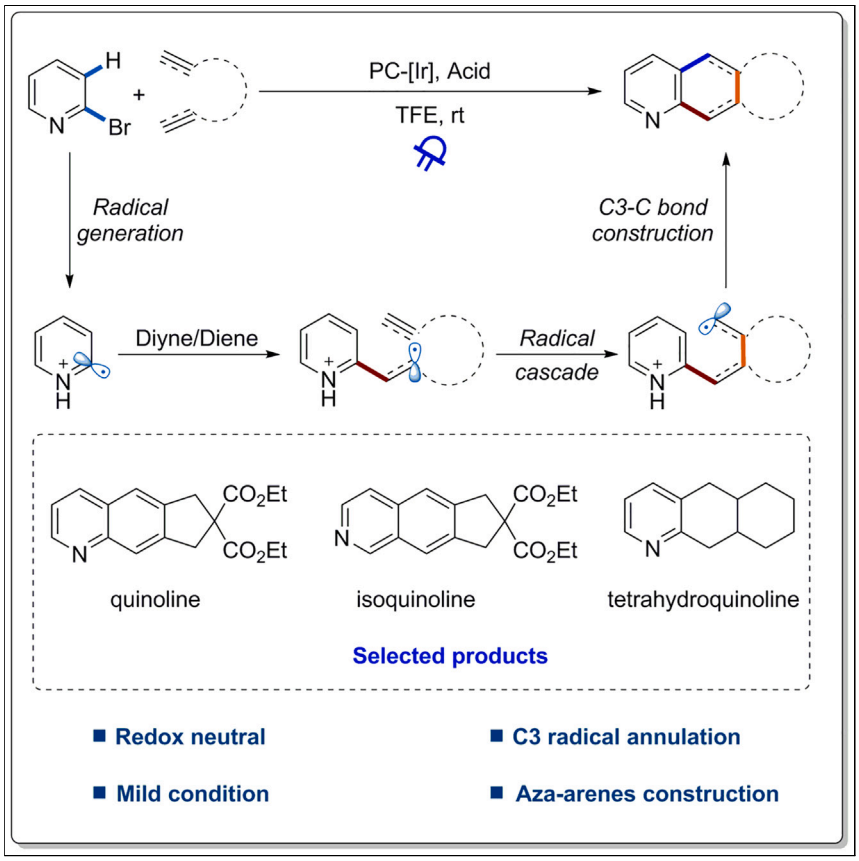

Pyridines, quinolines, and their derivatives contribute to a big drug market. However, most methods for quinoline synthesis usually initiate from aromatic cycles rather than pyridines. Here, He et al. describe a visible-light-induced catalytic construction of tricyclic quinolines or tetrahydroquinolines from halopyridines.

Gu-Cheng He, Ting-Ting Song, Xiang-Xin Zhang, ..., Boshun Wan, Shi-Yu Guo, Qing-An Chen

carlosguo10@dicp.ac.cn (S.-Y.G.)
qachen@dicp.ac.cn (Q.-A.C.)

Highlights

Generation of pyridyl radical via oxidative quenching

Radical cascade reaction of alkenes/alkynes

Construction of aza-arenes from halopyridines

Prolific synthetic transformations

He et al., Chem Catalysis 3, 100793
November 16, 2023
https://doi.org/10.1016/j.checat.2023.100793

Please cite this article in press as: He et al., Visible-light-induced catalytic construction of tricyclic aza-arenes from halopyridines, Chem Catalysis (2023), https://doi.org/10.1016/j.checat.2023.100793

Chem Catalysis

CellPress

Article

Visible-light-induced catalytic construction of tricyclic aza-arenes from halopyridines

Gu-Cheng He,[1,2] Ting-Ting Song,[1] Xiang-Xin Zhang,[1,2] Yan Liu,[1,2] Xiao-Yu Wang,[1,2] Boshun Wan,[1,2] Shi-Yu Guo,[1,*] and Qing-An Chen[1,2,3,*]

SUMMARY

Pyridines and quinolines are prevalent aza-arene motifs existing in drugs and natural products. It is of great interest to develop a more step- and atom-economy strategy for the construction of quinolines from more accessible pyridines. Herein, a visible-light-induced intermolecular cascade cyclization is developed for the coupling of halopyridies with diynes or dienes to construct tricyclic aza-arenes. Mechanistic studies indicate that the reaction processes include pyridyl radical generation, radical cascade addition, and cyclization processes. A series of fused-ring aza-arenes, such as quinoline, isoquinoline, and 5,6,7,8-tetrahydroquinoline, could be obtained via this protocol. Scale-up reaction and further transformations demonstrate the synthetic utility of this approach.

INTRODUCTION

As two important heterocycles, pyridines and quinolines play great roles in organic synthesis, catalysis, natural product, pharmaceutical, materials, etc.[1–4] Among top 200 small molecule drugs by retail sales in 2022,[5] pyridines, quinolines, and their derivatives, such as Trikafta, Ibrance, Rexulti, and Lenvima, contributed a market of more than $75 billion (Figure 1A). Given the abundance and importance of nitrogen heterocycles,[6–12] it is of great interest to construct quinolines directly from pyridines. And from the point of view of their chemical structure, it should be easy to realize this proposal. However, the relevant reports on converting pyridines to quinolines are surprisingly very limited.

In 2002, Takahashi and co-workers reported coupling reactions of stoichiometric amount of zirconacyclopentadienes with 2-bromo-3-iodopyridine to synthesize quinolines (Figure 1B).[13] And, the utilization of excess CuCl, n-BuLi, and DMPU further limited its applicability. Until 2011, Li and co-workers reported Rh-catalyzed oxidative annulation of pyridines to synthesize quinolines under 120°C (Figure 1C).[14] This strategy involved C−H activation and cyclization processes, which required the assistance of pre-installed directing groups and the utilization of equivalent copper(II) oxidants. Considering the starting materials used above are not readily available and considering the restriction of metal catalysis in handling nitrogen-containing heteroarenes, it is of great importance to develop a new strategy for construction of quinolines from more accessible pyridines.

The past decade has witnessed the development of photocatalysis in radical cascade reactions.[15–20] Photocatalytic pyridine functionalizations have also been reported as a state-of-the-art technique in organic synthesis.[21–37] The azolyl radicals generation from halo-heteroaromatics via reductive quenching of photocatalysts

THE BIGGER PICTURE

Drugs containing skeletons of pyridines or quinolines possess a huge market among the top 200 small molecule drugs by retail sales in 2022. Given the abundance and importance of nitrogen heterocycles, it is of great interest to construct quinolines directly from pyridines. Here, a visible-light-induced catalytic construction of tricyclic quinolines or tetrahydroquinolines from halopyridines was reported. This protocol featured the generation of pyridyl radicals and the radical cascade process. Quenching experiments and cyclic voltammograms showed the significance of acid in the reactions. Synthetic transformations proved the practicality of this protocol.

Please cite this article in press as: He et al., Visible-light-induced catalytic construction of tricyclic aza-arenes from halopyridines, Chem Catalysis (2023), https://doi.org/10.1016/j.checat.2023.100793

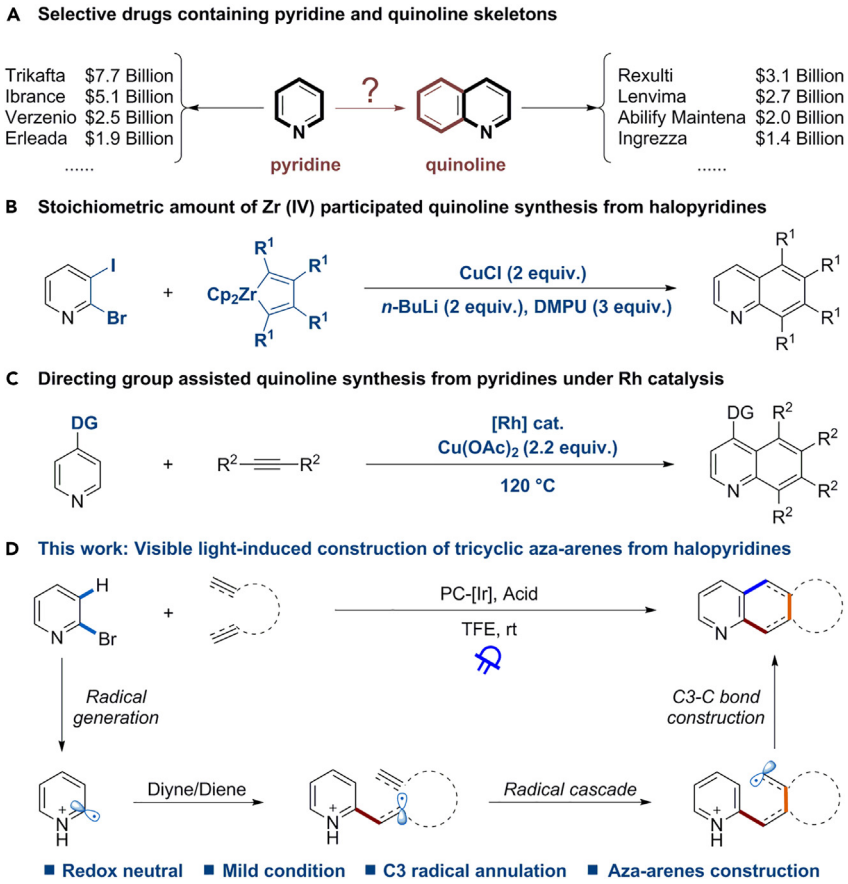

Figure 1. Representative pyridines/quinolines and the strategies for quinoline synthesis from pyridines

(A) Selective drugs containing pyridine and quinoline skeletons.

(B) Stoichiometric amount of Zr (IV) participated quinoline synthesis from halopyridines.

(C) Directing group assisted quinoline synthesis from pyridines under Rh catalysis.

(D) Visible light-induced construction of tricyclic aza-arenes from halopyridines.

were developed by Stephenson, Jui, Weaver, and others.[38–47] Hydroarylation of alkenes/alkynes could be realized via these protocols. Inspired by these precedents and our continued interest in photocatalysis,[48–53] we envisioned that the quinolines could be constructed from halopyridines under mild photocatalysis. Herein, we report a visible-light-induced construction of quinolines straight from halopyridines (Figure 1D). The pyridyl radicals could be generated under acidic environment via photocatalytic activation of halopyridines. Further radical cascade with diynes/dienes could deliver vinyl radicals/alkyl radicals, which would undergo C3−C bond formation with pyridines to provide the desired products. This strategy features redox neutral, mild condition, C3 radical annulation, and aza-arenes construction. And it provides an important complement for traditional quinoline synthesis.[54–62]

RESULTS AND DISCUSSION

Initially, 2-bromopyridine (**1a**) and diethyl 2,2-di(prop-2-yn-1-yl)malonate (**2a**) were selected as the model substrates to test our hypothesis (Table 1). When using $[Ir(ppy)_2(dtbbpy)]PF_6$ as the photocatalyst, trifluoroacetic acid (TFA) as acid, and trifluoroethanol (TFE) as the solvent, the fused-ring construction could deliver the

[1]Dalian Institute of Chemical Physics, Chinese Academy of Sciences, Dalian 116023, People's Republic of China

[2]University of Chinese Academy of Sciences, Beijing 100049, People's Republic of China

[3]Lead contact

*Correspondence: carlosguo10@dicp.ac.cn (S.-Y.G.), qachen@dicp.ac.cn (Q.-A.C.)

https://doi.org/10.1016/j.checat.2023.100793

Please cite this article in press as: He et al., Visible-light-induced catalytic construction of tricyclic aza-arenes from halopyridines, Chem Catalysis (2023), https://doi.org/10.1016/j.checat.2023.100793

Table 1. Optimization of the reaction conditions

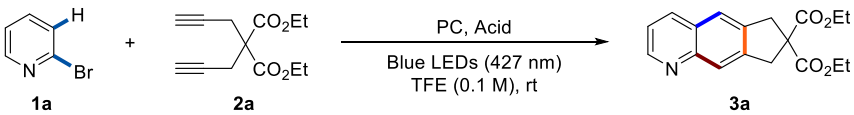

Entry[a]	Photocatalyst (PC)	Acid	Solvent	Yield 3a (%)
1	$[Ir(ppy)_2(dtbbpy)]PF_6$	TFA	TFE	56
2	$[Ir(dF(CF_3)ppy)_2(dtbbpy)]BF_4$	TFA	TFE	27
3	$Ir(ppy)_3$	TFA	TFE	18
4	$Ru(bpy)_3Cl_2 \cdot 6H_2O$	TFA	TFE	–
5[b]	4CzIPN	TFA	TFE	16
6	$[Ir(ppy)_2(dtbbpy)]PF_6$	$PhCO_2H$	TFE	18
7	$[Ir(ppy)_2(dtbbpy)]PF_6$	TsOH	TFE	23
8	$[Ir(ppy)_2(dtbbpy)]PF_6$	TFA	MeOH	–
9	$[Ir(ppy)_2(dtbbpy)]PF_6$	TFA	MeCN	–
10	$[Ir(ppy)_2(dtbbpy)]PF_6$	TFA	DCM	–
11	$[Ir(ppy)_2(dtbbpy)]PF_6$	TFA	HFIP	48
12[c]	$[Ir(ppy)_2(dtbbpy)]PF_6$	TFA	TFE	77 (73)[d]
13[c]	–	TFA	TFE	–
14[c]	$[Ir(ppy)_2(dtbbpy)]PF_6$	–	TFE	27

[a]Reaction conditions: **1a** (0.20 mmol), **2a** (0.40 mmol), photocatalyst (2 mol %), acid (0.40 mmol), solvent (2.0 mL), blue LEDs (427 nm, 40 W), RT, 24 h, yields determined by GC-FID using 1,3,5-trimethoxybenzene as the internal standard.
[b]5 mol % 4CzIPN.
[c]0.80 mmol **2a**.
[d]Isolated yield.

product with 56% yield under the irradiation of blue LEDs for 24 h. Switching to other photocatalysts, such as $[Ir(dF(CF_3)ppy)_2(dtbbpy)]BF_4$, $Ir(ppy)_3$, $Ru(bpy)_3Cl_2 \cdot 6H_2O$, and 4CzIPN, the reactivity was inhibited (entries 1–5). Other Brønsted acids like $PhCO_2H$ or TsOH delivered the target products with low yields (entries 6–7). Afterward, the evaluation of solvent found that the reaction could not proceed in other solvents like methanol, acetonitrile, or dichloromethane (entries 8–10). Similar to TFE, hexafluoro-2-propanol (HFIP) could also be used as solvent for this reaction (entry 11). To our delight, a higher concentration of diyne **2a** delivered desired product **3a** with a decent yield of 77% (entry 12). Finally, control experiments were conducted under the standard condition without photocatalyst or acid (entries 13 and 14). No target product could be obtained in the absence of photocatalyst, which indicated the indispensable role of photocatalysis. Interestingly, the reaction could also provide the product without the use of a Brønsted acid, perhaps owing to the acidity of strong protonic solvent TFE.

Subsequently, the scope of pyridines was investigated under the optimized conditions (Figure 2). A wide range of substituted 2-halo-pyridines were applied and transformed to target tricyclic aza-arene products (**3a–3o**). Notably, when 2-bromopyridine (**1a**) was switched to chloro-substitution, only a moderate yield could be achieved. And for 2-iodopyridine, the reaction was a mess, where only a trace amount of product was observed. The methyl substituents at different positions of 2-bromopyridines were tolerated to deliver the desired products (**3b–3d**). Bromopyridines with *N*-acetamide or methoxy groups also showed good performance in this transformation (**3f–3h, 3n,** and **3o**). Especially, the utilization of catalytic amount of aluminum chloride would deliver **3h** with a higher yield (from 50% to 65%). The product structure of **3h** was confirmed by single crystal X-ray diffraction.

Please cite this article in press as: He et al., Visible-light-induced catalytic construction of tricyclic aza-arenes from halopyridines, Chem Catalysis (2023), https://doi.org/10.1016/j.checat.2023.100793

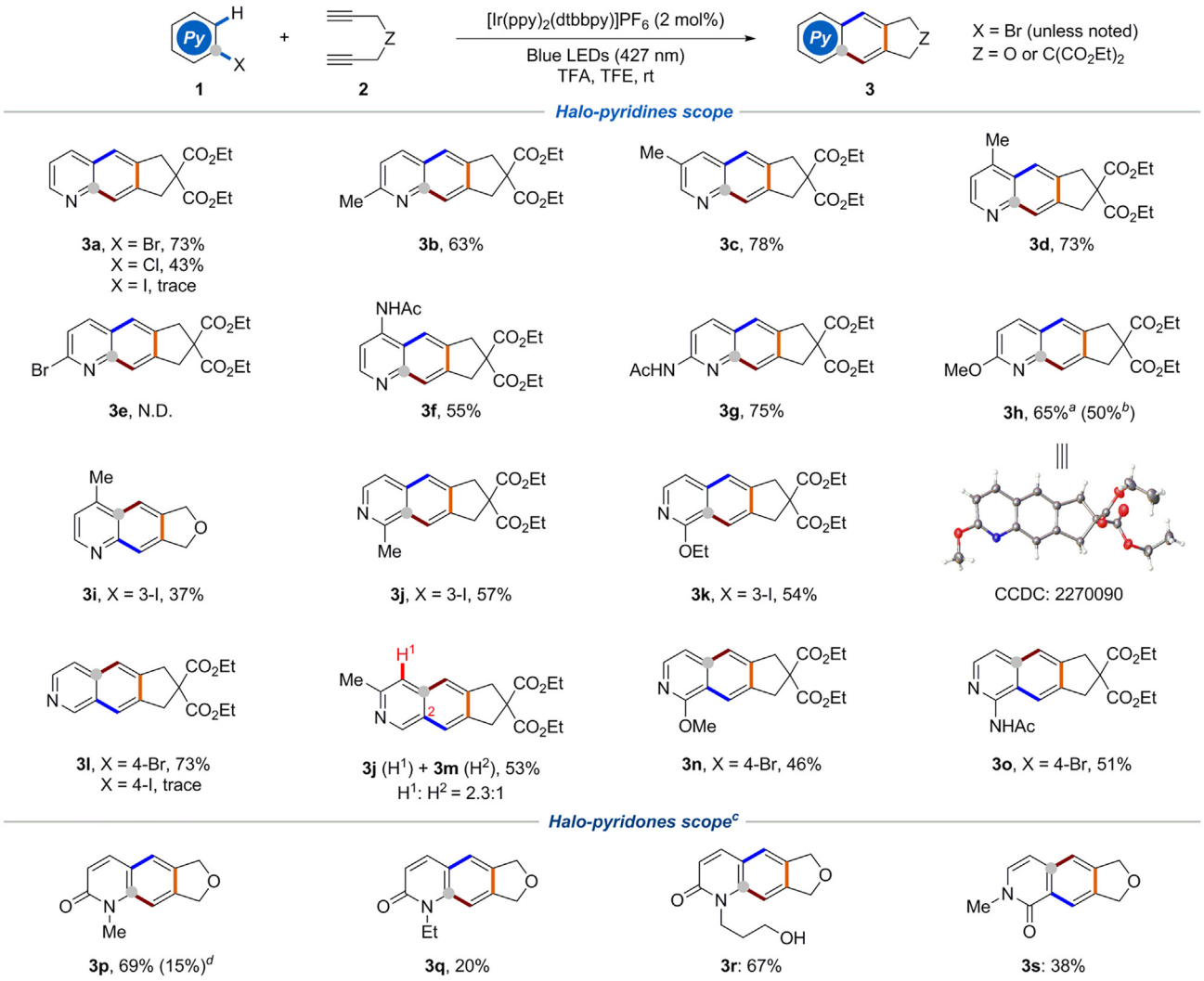

Figure 2. Substrate scope with respect to pyridines

Conditions: **1** (0.20 mmol), **2** (0.80 mmol), $[Ir(ppy)_2(dtbbpy)]PF_6$ (2 mol %), TFA (0.40 mmol), TFE (2.0 mL), blue LEDs (427 nm, 40 W), RT, 24 h. [a]**2** (1.40 mmol), $AlCl_3$ (20 mol %) instead of TFA, 48 h. [b]48 h. [c]**2** (1.0 mmol), $Zn(OTf)_2$ (0.10 mmol). [d]Yield in the parentheses was under the standard condition.

However, electron withdrawing groups, such as 2,6-dibromopyridine, were not suitable in this condition (**3e**). Then, we turned to explore halo substituents at meta or para positions. To our delight, 3-iodo-pyridines could be transformed to corresponding quinoline or isoquinoline products in moderate yields (**3i–3k**). Although 4-iodo-pyridine failed, 4-bromo-pyridine could react smoothly and gave the desired product in 73% yield (**3l**). 4-Bromo-2-methylpyridine could deliver the corresponding product with a low regioselectivity at 3 and 5 positions (**3j** and **3m**). These results also indicate a reaction tendency at the ortho position of EDG groups rather than para position (**3j–3o**). This regioselectivity probably resulted from the stabilized effect of the *ortho*-EDG group on the generated dearomatized radical intermediate. Based on our previous experience,[51] we were delighted to find that pyridone substrates could also deliver the target quinolinone products with the additive of zinc triflate (**3p–3s**). The addition of zinc triflate could provide **3p** with higher yield, probably because the coordination of zinc ions could help the transformation from pyridone to pyridinium cation.

Please cite this article in press as: He et al., Visible-light-induced catalytic construction of tricyclic aza-arenes from halopyridines, Chem Catalysis (2023), https://doi.org/10.1016/j.checat.2023.100793

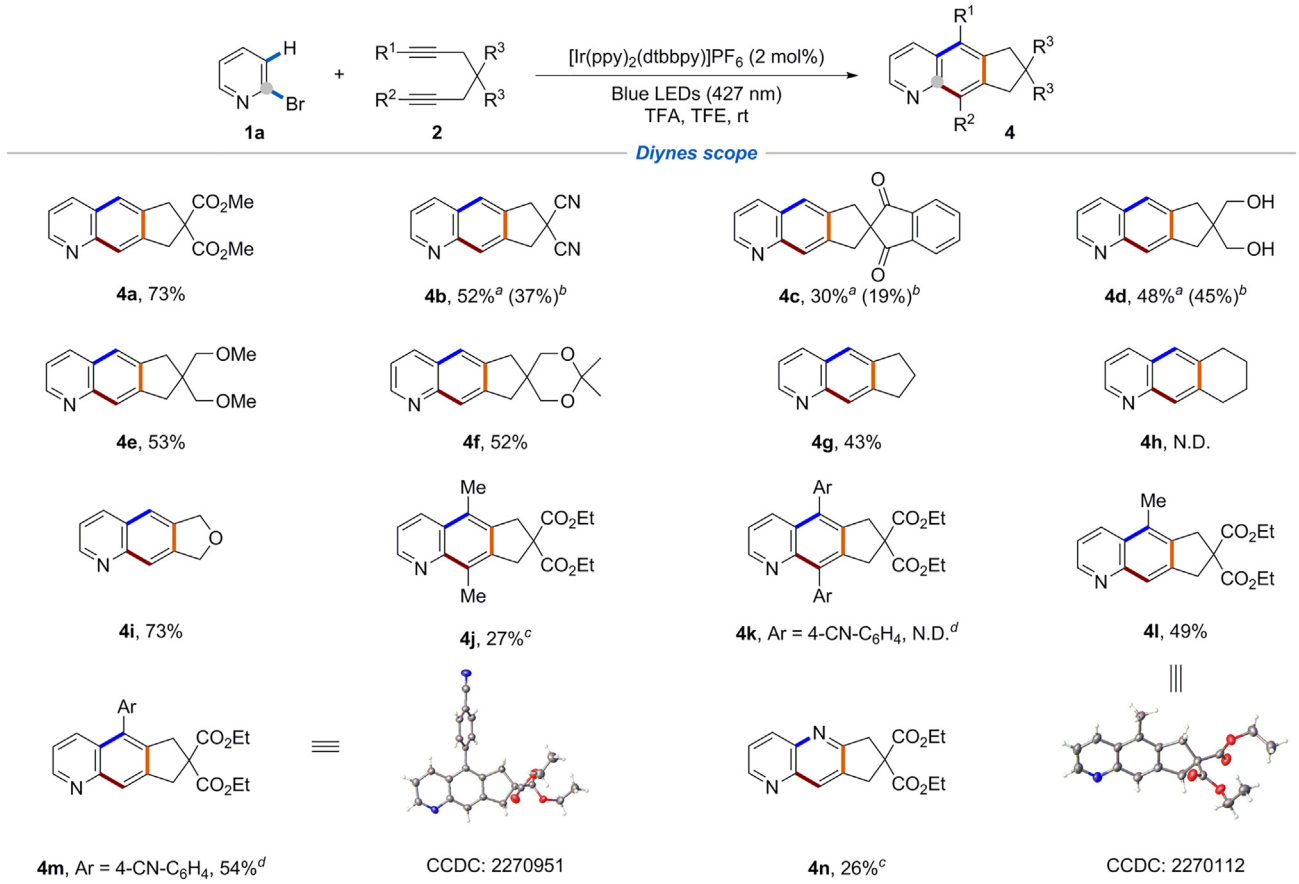

Figure 3. Substrate scope with respect to alkynes

Conditions: **1a** (0.20 mmol), **2** (0.80 mmol), $[Ir(ppy)_2(dtbbpy)]PF_6$ (2 mol %), TFA (0.40 mmol), TFE (2.0 mL), blue LEDs (427 nm, 40 W), RT, 24 h. [a]**2** (1.0 mmol), $AlCl_3$ (20 mol %) instead of TFA, 48 h. [b]Yields in the parentheses were under the standard condition. [c]**2** (1.4 mmol). [d]**2** (1.0 mmol).

The diynes scope was examined under the standard condition (Figure 3). Diynes with dimethyl malonate group could deliver the desired product with 74% yield (**4a**). For diynes with electron-deficient groups, such as cyano group, a medium yield could also be achieved (**4b**) when switching to use a catalytic amount of aluminum chloride. Substrate bearing indanedione group was also tolerated, providing a fused-ring quinoline with an additional spiro ring (**4c**). With respect to hydroxymethyl group or methoxymethyl group, the desired products could be obtained with moderate yields (**4d** and **4e**). Another product with spiro ring (**4f**) could also be delivered smoothly. For 1,6-heptadiyne, a lower yield was observed probably owing to the absence of Thorpe-Ingold effect (**4g**). This method could not be applicable for 1,7-octadiyne because the radical cascade process might be harder (**4h**). Propargyl ether could provide the corresponding product with a higher yield (**4i**, 73%) when comparing with 1,6-heptadiyne (**4g**, 43%). As for substrates with internal alkynes (**4j** and **4k**), they showed inhibited reactivity when comparing with terminal alkynes. Interestingly, the method was successfully applied to unsymmetric mono-substituted diynes (**4l** and **4m**). The regio configuration of products **4l** and **4m** were unambiguously confirmed by single crystal X-ray diffraction. These results showed that the initial generated pyridyl radical prefer to undergo addition onto terminal alkyne rather than internal alkyne. Besides, it is interesting to find that cyano groups could be applicable in the radical cascade process to deliver the 1,5-naphthyridine product (**4n**).

Please cite this article in press as: He et al., Visible-light-induced catalytic construction of tricyclic aza-arenes from halopyridines, Chem Catalysis (2023), https://doi.org/10.1016/j.checat.2023.100793

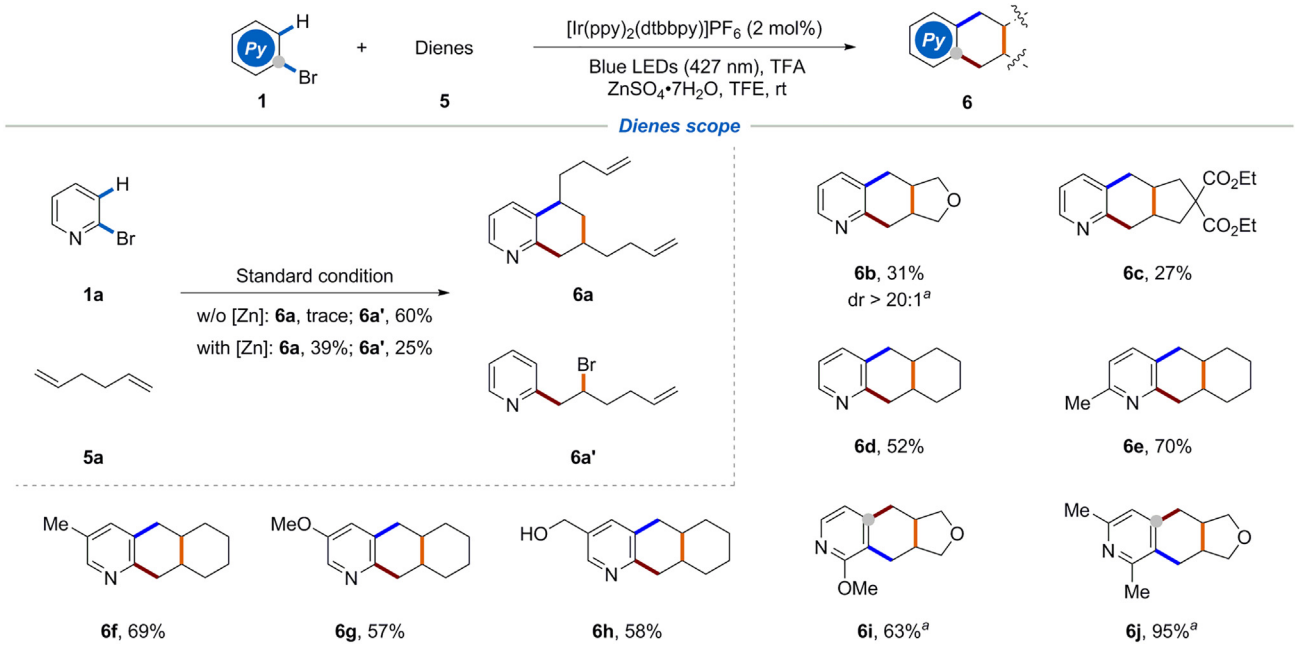

Figure 4. Catalytic construction of tetrahydro(iso)quinolines from dienes

Conditions: **1** (0.20 mmol), **5** (1.0 mmol), $[Ir(ppy)_2(dtbbpy)]PF_6$ (2 mol %), TFA (0.40 mmol), $ZnSO_4 \cdot 7H_2O$ (10 mol %), TFE (4.0 mL), blue LEDs (427 nm, 40 W), RT, 24 h. Unless noted, the diastereoselectivity (dr) of **6** is 1:1∼3:1. [a]48 h.

Next, we examined dienes scope (Figure 4). 2-Bromopyridine (**1a**) and 1,5-hexadiene (**5a**) were selected to test the protocol. The fused-ring construction could not be observed under the former reaction condition due to the high ring strain of the proposed product. However, a trace amount of the three-component cascade product (**6a**) could be delivered along with the halopyridylation side product (**6a′**). A Lewis acid such as zinc sulfate could promote the alkyl radical cascade process and partially inhibit the formation of side product **6a'**. The zinc ions might coordinate with nitrogen atom and stabilize the desired reaction intermediate. When switching to bisallyl ether, a moderate yield could be delivered with an excellent diastereomeric selectivity (**6b**). Malonate group could also be tolerated under this method (**6c**). When turning to octadiene, products could be obtained with a moderate yield (**6d**). Methyl substitution on pyridines provided higher reactivities (**6e** and **6f**). Also, methoxy and hydroxymethyl groups could afford the desired products with moderate yields (**6g** and **6h**). Besides, tetrahydroisoquinolines could also be obtained when subjecting 4-bromo pyridines to this strategy (**6i** and **6j**).

With the intention to understand the mechanism of this protocol, preliminary mechanistic experiments were conducted (Figure 5). The light on/off experiments showed the necessity of blue LED irradiation (Figure 5A). Then Stern-Volmer quenching experiments were further carried out to figure out the quenching species (Figure 5B). The protonated halopyridines (**1a**) could effectively quench the excited iridium photocatalyst with a Stern-Volmer constant of 5.99 mL/mmol, while diynes (**2a**) showed no quenching effect. Due to the special fluorescence of the product (**3a**) under the irradiation, ultraviolet-visible-light absorption experiments were conducted (Figure 5C). Compound **3a** exhibited a good absorption of ultraviolet light, while the absorption curve of protonated **3a** showed an obvious redshift to the visible-light region, especially blue light. Subsequently, the absorption curve of iridium

Please cite this article in press as: He et al., Visible-light-induced catalytic construction of tricyclic aza-arenes from halopyridines, Chem Catalysis (2023), https://doi.org/10.1016/j.checat.2023.100793

CellPress

A Light on/off experiments

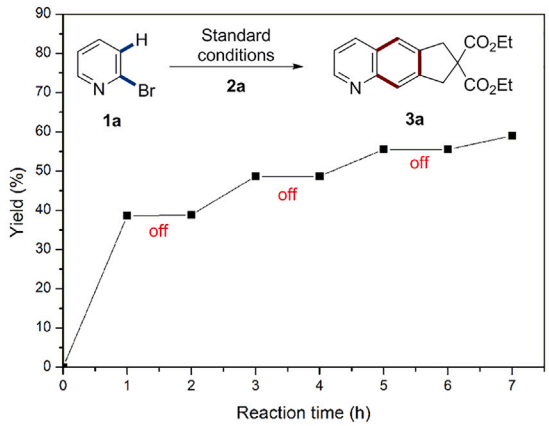

B Stern-Volmer quenching studies

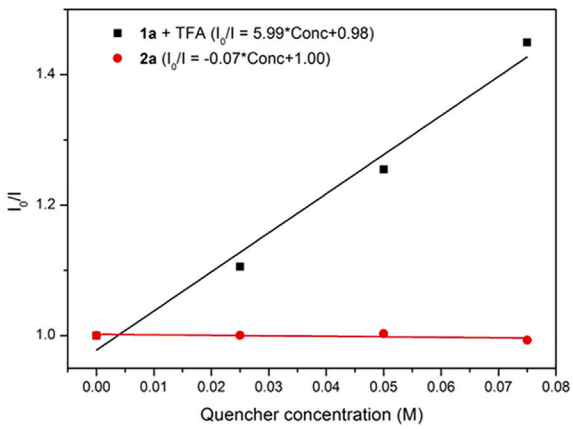

C UV-vis absorption spectrum

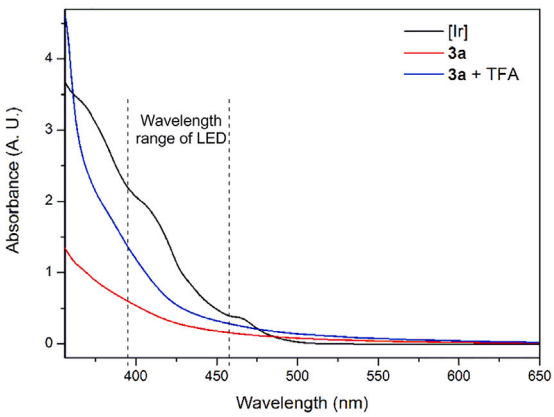

D The feedback of 3a on the reaction efficiency

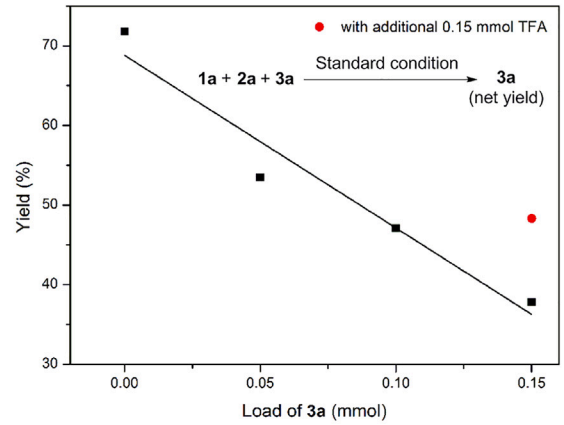

E Radical trapping experiments

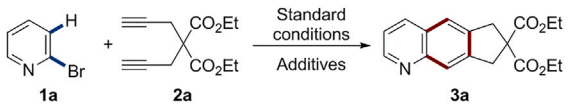

entry	Additives	Yield of **7a**	Yield of **3a**
1	None	-	73%
2	TEMPO (1.5 eq.)	-	48%
3	BHT (1.5 eq.)	29%	18%

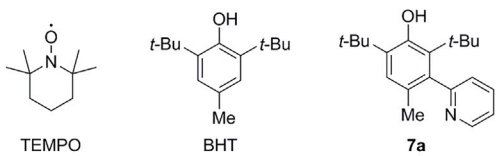

F Cyclic voltammograms (vs. SCE)

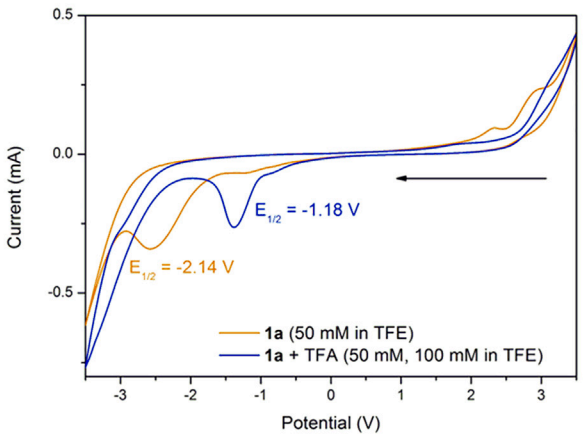

Figure 5. Mechanistic investigations

(A) Light on/off experiments.
(B) Stern-Volmer quenching studies.
(C) UV-vis absorption spectrum.
(D) The feedback of **3a** on the reaction efficiency.
(E) Radical trapping experiments.
(F) Cyclic voltammograms (vs. SCE).

Please cite this article in press as: He et al., Visible-light-induced catalytic construction of tricyclic aza-arenes from halopyridines, Chem Catalysis (2023), https://doi.org/10.1016/j.checat.2023.100793

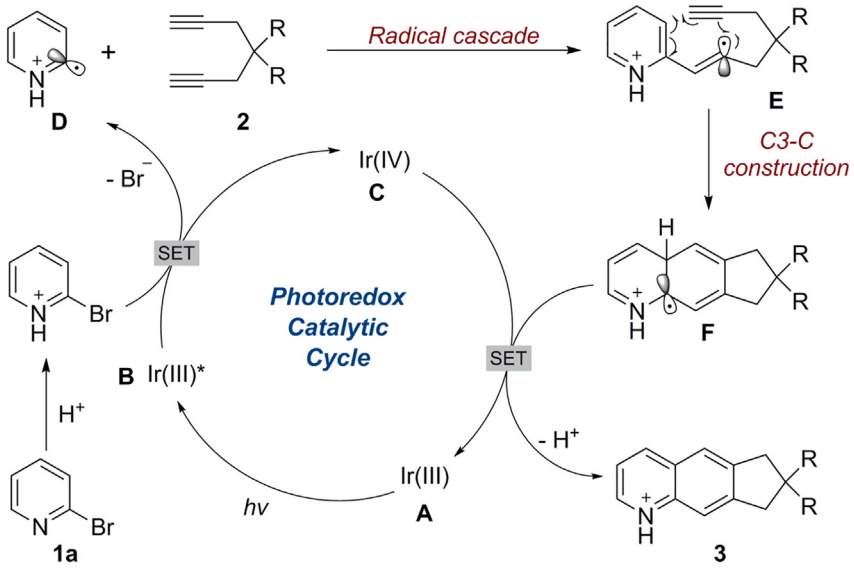

Figure 6. Proposed mechanism

photocatalyst (molar ratio of [Ir]: **3a** = 2:100) indicated that product **3a** might have a competitive relationship with photocatalyst in terms of light absorption. Therefore, parallel experiments with gradient addition of **3a** were performed to evaluate the product's impact on reactivity (Figure 5D). As indicated by the results, the yield of the reaction would be inhibited by the addition of **3a**. The addition of extra TFA could not fully restore the reactivity. These results suggest the strong product inhibition effect on the reactivity probably resulted from its competition with the photocatalyst for light absorption.

Afterward, radical trapping reactions were completed (Figure 5E). The addition of TEMPO or BHT would inhibit the reaction. And the pyridyl radical could be captured by BHT to deliver compound **7a**. Cyclic voltammograms were also conducted with different species to gain mechanistic insight (Figure 5F). Bromopyridine **1a** (50.0 mM in TFE, with $TBAPF_6$ 0.10 M) exhibited an apparent peak with the redox potential at −2.14 V (Figure 5F, orange curve). With the addition of TFA (100.0 mM), the redox potential of **1a** (50.0 mM in TFE, with $TBAPF_6$ 0.1 M) shifted to −1.18 V (Figure 5F, blue curve). These results suggested that the protonation of pyridines make it easier to be reduced.

Based on the experimental results mentioned above, a plausible mechanism was proposed (Figure 6). Photosensitive Ir(III) complex **A** is irradiated under blue light to give excited Ir(III)* species **B**. Protonated pyridine **1a** is reduced by the excited iridium photocatalyst **B** to generate the pyridyl radical **D** and oxidative Ir(IV) **C**. The electrophilic intermediate **D** is captured intermolecularly by the diyne **2**, forming the nucleophilic vinyl radical **E**. A subsequent intramolecular radical cascade addition delivers a cyclized dearomatization intermediate **F**. And a final oxidation of intermediate **F** by the high valent iridium complex **C** facilitates the elimination of proton to provide the rearomatization product **3**. Furthermore, the corresponding quantum yield (Φ) has been subsequently determined as 0.85, which might exclude the radical chain pathway (see the supplemental information for details).

Please cite this article in press as: He et al., Visible-light-induced catalytic construction of tricyclic aza-arenes from halopyridines, Chem Catalysis (2023), https://doi.org/10.1016/j.checat.2023.100793

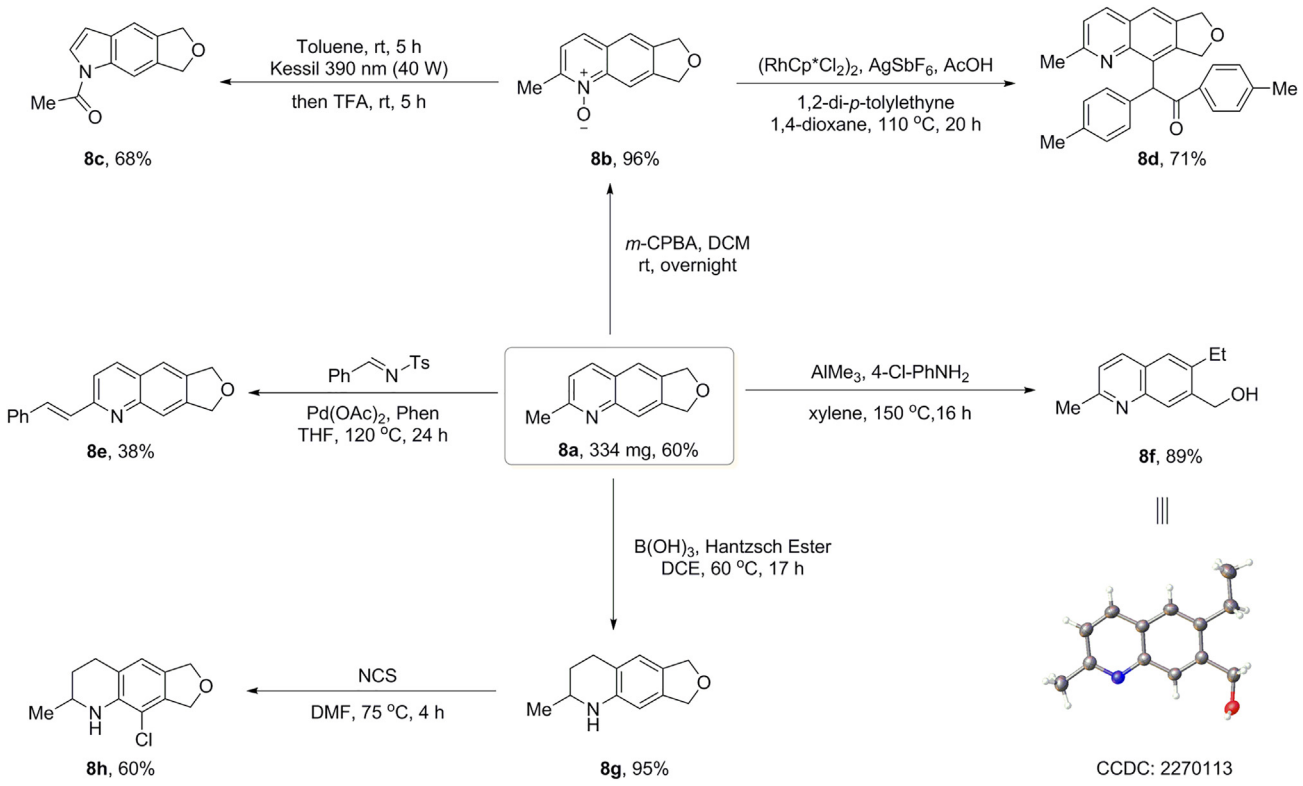

Figure 7. Scale-up reaction and synthetic applications

Finally, scale-up reaction and synthetic transformations were performed to demonstrate the synthetic utility of this protocol (Figure 7). A 3.0 mmol scale reaction using 2-bromo-6-methylpyridine and dipropargyl ether as substrate was conducted to deliver product **8a** in 60% yield. Quinoline *N*-oxide **8b** could be easily obtained with a high yield using *m*-CPBA under a mild condition.[63] From quinoline *N*-oxide, a skeletal editing reaction could produce *N*-acylindole with a decent yield under the irradiation of 390-nm LEDs (**8c**).[64] To our delight, a sp^2 C−H activation at C8 position of quinoline could be conducted with 71% yield under rhodium catalysis (**8d**).[65] Through a sp^3 C−H functionalization pathway, 2-methyl group was alkenylated smoothly under palladium catalysis (**8e**).[66,67] Meanwhile, the dihydrofuran ring could be opened via the activation of $AlMe_3$ with single regioselectivity (**8f**).[68] The structure of **8f** was unambiguously determined by single crystal X-ray diffraction. As a supplement of our quinoline synthesis, 1,2,3,4-terahydroquinoline could be obtained through a selective transfer hydrogenation in the presence of Hantzsch ester (**8g**).[69] Finally, 1,2,3,4-terahydroquinoline **8g** could be further selectively chlorinated by NCS (**8h**).[70]

Conclusion

In conclusion, we have developed a protocol for step-economy construction of quinolines from halopyridines under photocatalysis. Symmetric and unsymmetric skipped diynes or dienes could be used to selectively trap the generated pyridyl radical for the formation of fused rings. This strategy features redox neutral, mild condition and C3 radical annulation of pyridines. Several tricyclic aza-arenes including quinolines, isoquinolines, and 5,6,7,8-tetrahydroquinolines could be obtained via this strategy. Scale-up reaction and transformations further

Please cite this article in press as: He et al., Visible-light-induced catalytic construction of tricyclic aza-arenes from halopyridines, Chem Catalysis (2023), https://doi.org/10.1016/j.checat.2023.100793

demonstrated the synthetic utility of this protocol. Further investigation about pyridyl radicals has been on the schedule in our laboratory.

EXPERIMENTAL PROCEDURES

Resource availability

Lead contact

Further information and requests for resources and reagents should be directed to and will be fulfilled by the lead contact, Qing-An Chen (qachen@dicp.ac.cn).

Materials availability

Commercially available reagents were used without further purification. Other solvents were treated prior to use according to the standard methods. Unless otherwise stated, all reactions were conducted under an inert atmosphere using standard Schlenk techniques or in a nitrogen-filled glovebox. ^{1}H nuclear magnetic resonance (NMR) and ^{13}C NMR spectra were recorded at room temperature in $CDCl_3$ on 400- or 700-MHz instruments with tetramethylsilane as the internal standard. Flash column chromatography was performed on silica gel (200–300 mesh). All reactions were monitored by thin-layer chromatography, NMR, or gas chromatography with flame-ionization detection (GC-FID) analysis. High-resolution mass spectrometry (HRMS) data were obtained with a Micromass HPLC-Q-TOF mass spectrometer (electrospray ionization) or Agilent 6540 Accurate-MS spectrometer (quadrupole time of flight [Q-TOF]).

Data and code availability

The authors declare that data supporting the findings of this study are available within the article and the supplemental information. Crystallographic data for the structures reported in this article have been deposited at the Cambridge Crystallographic Data Center (CCDC) under CCDC: 2270090 (**3h**), 2270112 (**4l**), 2270951 (**4m**), and 2270113 (**8f**). Copies of the data can be obtained free of charge from https://www.ccdc.cam.ac.uk/structures/. More crystal details could be obtained in the supplemental information (S27–S30) and individual files (3h.cif, 3h-checkcif.pdf, 4l.cif, 4l-checkcif.pdf, 4m.cif, 4m-checkcif.pdf, 8f.cif, 8f-checkcif.pdf). Details about experimental procedures and characterization data of products (NMR, HRMS) can be found in the supplemental information (S7–S15). Failed substrate scope can be seen in supplemental information (S16). Mechanistic studies can be found in the supplemental information (S17–S23). Scale-up reaction and synthetic transformations can be obtained in the supplemental information (S24–S26). Copies of NMR spectra can be seen in the supplemental information (S31–S94). All other data are available from the lead contact upon reasonable request.

SUPPLEMENTAL INFORMATION

Supplemental information can be found online at https://doi.org/10.1016/j.checat.2023.100793.

ACKNOWLEDGMENTS

Financial support from the National Natural Science Foundation of China (22271277, 21971234, and 22301299) and the Doctoral Research Startup Fund Project of Liaoning Province (2020BS017) is acknowledged.

AUTHOR CONTRIBUTIONS

Q.-A.C. and S.-Y.G. conceived and supervised the project. Q.-A.C. and G.-C.H. designed the experiments. G.-C.H., T.-T.S., X.-X.Z., Y.L., and X.-Y.W. performed the

experiments and analyzed the data. All authors discussed the results and commented on the manuscript.

DECLARATION OF INTERESTS

The authors declare no competing interests.

Received: July 27, 2023
Revised: September 11, 2023
Accepted: October 10, 2023
Published: November 1, 2023

REFERENCES

1. Vitaku, E., Smith, D.T., and Njardarson, J.T. (2014). Analysis of the structural diversity, substitution patterns, and frequency of nitrogen heterocycles among U.S. FDA approved pharmaceuticals. J. Med. Chem. *57*, 10257–10274. https://doi.org/10.1021/jm501100b.

2. Bhutani, P., Joshi, G., Raja, N., Bachhav, N., Rajanna, P.K., Bhutani, H., Paul, A.T., and Kumar, R. (2021). U.S. FDA Approved Drugs from 2015-June 2020: A Perspective. J. Med. Chem. *64*, 2339–2381. https://doi.org/10.1021/acs.jmedchem.0c01786.

3. Matada, B.S., Pattanashettar, R., and Yernale, N.G. (2021). A comprehensive review on the biological interest of quinoline and its derivatives. Bioorg. Med. Chem. *32*, 115973. https://doi.org/10.1016/j.bmc.2020.115973.

4. Shearer, J., Castro, J.L., Lawson, A.D.G., MacCoss, M., and Taylor, R.D. (2022). Rings in Clinical Trials and Drugs: Present and Future. J. Med. Chem. *65*, 8699–8712. https://doi.org/10.1021/acs.jmedchem.2c00473.

5. Top 200 SMALL Molecule Drugs by Sales in 2022. https://njardarson.lab.arizona.edu/sites/njardarson.lab.arizona.edu/files/NjardarsonGroup2022SmallMoleculeTopPosterV3.pdf.

6. Singh, P. (2022). Recent Developments in the Synthesis and Applications of Pyridines (Elsevier).

7. Zhang, B., Zhou, Q., Chen, R., and Jiang, H. (2012). Transition-Metal-Catalyzed Functionalization of Pyridines. Chin. J. Org. Chem. *32*, 1653–1665. https://doi.org/10.6023/cjoc1201291.

8. Murakami, K., Yamada, S., Kaneda, T., and Itami, K. (2017). C-H Functionalization of Azines. Chem. Rev. *117*, 9302–9332. https://doi.org/10.1021/acs.chemrev.7b00021.

9. Proctor, R.S.J., and Phipps, R.J. (2019). Recent Advances in Minisci-Type Reactions. Angew. Chem. Int. Ed. *58*, 13666–13699. https://doi.org/10.1002/anie.201900977.

10. Sun, A.C., McAtee, R.C., McClain, E.J., and Stephenson, C.R.J. (2019). Advancements in Visible-Light-Enabled Radical C(sp)2-H Alkylation of (Hetero)arenes. Synthesis *51*, 1063–1072. https://doi.org/10.1055/s-0037-1611658.

11. Failla, M., Lombardo, G.W., Orlando, P., Fiorito, D., Bombonato, E., Ronchi, P., Passarella, D., and Fasano, V. (2023). Late-Stage Functionalisation of Pyridine-Containing Bioactive Molecules: Recent Strategies and Perspectives. Eur. J. Org. Chem. *26*, e202300074. https://doi.org/10.1002/ejoc.202300074.

12. Josephitis, C.M., Nguyen, H.M.H., and McNally, A. (2023). Late-Stage C-H Functionalization of Azines. Chem. Rev. *123*, 7655–7691. https://doi.org/10.1021/acs.chemrev.2c00881.

13. Takahashi, T., Li, Y., Stepnicka, P., Kitamura, M., Liu, Y., Nakajima, K., and Kotora, M. (2002). Coupling reaction of zirconacyclopentadienes with dihalonaphthalenes and dihalopyridines: a new procedure for the preparation of substituted anthracenes, quinolines, and isoquinolines. J. Am. Chem. Soc. *124*, 576–582. https://doi.org/10.1021/ja016848k.

14. Song, G., Gong, X., and Li, X. (2011). Synthesis of quinolines via Rh(III)-catalyzed oxidative annulation of pyridines. J. Org. Chem. *76*, 7583–7589. https://doi.org/10.1021/jo201266u.

15. Bonilla, P., Rey, Y.P., Holden, C.M., and Melchiorre, P. (2018). Photo-Organocatalytic Enantioselective Radical Cascade Reactions of Unactivated Olefins. Angew. Chem. Int. Ed. *57*, 12819–12823. https://doi.org/10.1002/anie.201808183.

16. Fuentes, N., Kong, W., Fernández-Sánchez, L., Merino, E., and Nevado, C. (2015). Cyclization cascades via N-amidyl radicals toward highly functionalized heterocyclic scaffolds. J. Am. Chem. Soc. *137*, 964–973. https://doi.org/10.1021/ja5115858.

17. Yao, L., and Gui, J. (2022). Application of the Radical Polyene Cyclization Reaction in Natural Product Synthesis. Chin. J. Org. Chem. *42*, 2703–2714. https://doi.org/10.6023/cjoc202204044.

18. Huang, H.M., and Procter, D.J. (2016). Radical-Radical Cyclization Cascades of Barbiturates Triggered by Electron-Transfer Reduction of Amide-Type Carbonyls. J. Am. Chem. Soc. *138*, 7770–7775. https://doi.org/10.1021/jacs.6b04086.

19. Jiang, H., Seidler, G., and Studer, A. (2019). Carboamination of Unactivated Alkenes through Three-Component Radical Conjugate Addition. Angew. Chem. Int. Ed. *58*, 16528–16532. https://doi.org/10.1002/anie.201910926.

20. Xu, S.-M., Chen, J.-Q., Liu, D., Bao, Y., Liang, Y.-M., and Xu, P.-F. (2017). Aroyl chlorides as novel acyl radical precursors via visible-light photoredox catalysis. Org. Chem. Front. *4*, 1331–1335. https://doi.org/10.1039/c7qo00012j.

21. Li, B.-J., and Shi, Z.-J. (2011). Ir-catalyzed highly selective addition of pyridyl C–H bonds to aldehydes promoted by triethylsilane. Chem. Sci. *2*, 488–493. https://doi.org/10.1039/c0sc00419g.

22. Ye, M., Gao, G.L., Edmunds, A.J.F., Worthington, P.A., Morris, J.A., and Yu, J.Q. (2011). Ligand-promoted C3-selective arylation of pyridines with Pd catalysts: gram-scale synthesis of (+/-)-preclamol. J. Am. Chem. Soc. *133*, 19090–19093. https://doi.org/10.1021/ja209510q.

23. Wübbolt, S., and Oestreich, M. (2015). Catalytic Electrophilic C-H Silylation of Pyridines Enabled by Temporary Dearomatization. Angew. Chem. Int. Ed. *54*, 15876–15879. https://doi.org/10.1002/anie.201508181.

24. Hu, R.B., Sun, S., and Su, Y. (2017). Visible-Light-Induced Carbo-2-pyridylation of Electron-Deficient Alkenes with Pyridinium Salts. Angew. Chem. Int. Ed. *56*, 10877–10880. https://doi.org/10.1002/anie.201704385.

25. Markham, J.P., Wang, B., Stevens, E.D., Burris, S.C., and Deng, Y. (2019). ortho-Alkylation of Pyridine N-Oxides with Alkynes by Photocatalysis: Pyridine N-Oxide as a Redox Auxiliary. Chem. Eur J. *25*, 6638–6644. https://doi.org/10.1002/chem.201901065.

26. Xu, J.H., Wu, W.B., and Wu, J. (2019). Photoinduced Divergent Alkylation/Acylation of Pyridine N-Oxides with Alkynes under Anaerobic and Aerobic Conditions. Org. Lett. *21*, 5321–5325. https://doi.org/10.1021/acs.orglett.9b01940.

27. Zhang, W.B., Yang, X.T., Ma, J.B., Su, Z.M., and Shi, S.L. (2019). Regio- and Enantioselective C-H Cyclization of Pyridines with Alkenes Enabled by a Nickel/N-Heterocyclic Carbene Catalysis. J. Am. Chem. Soc. *141*, 5628–5634. https://doi.org/10.1021/jacs.9b00931.

28. Dong, J., Yue, F., Liu, J., Song, H., Liu, Y., and Wang, Q. (2021). Visible-light-mediated three-component Minisci reaction for heteroarylethyl alcohols synthesis. Green Chem. *23*, 7963–7968. https://doi.org/10.1039/d1gc02807c.

29. Zhang, T., Luan, Y.X., Lam, N.Y.S., Li, J.F., Li, Y., Ye, M., and Yu, J.Q. (2021). A directive Ni catalyst overrides conventional site selectivity in pyridine C-H alkenylation. Nat. Chem. *13*, 1207–1213. https://doi.org/10.1038/s41557-021-00792-1.

30. Boyle, B.T., Levy, J.N., de Lescure, L., Paton, R.S., and McNally, A. (2022). Halogenation of the 3-position of pyridines through Zincke imine intermediates. Science *378*, 773–779. https://doi.org/10.1126/science.add8980.

31. Cao, H., Cheng, Q., and Studer, A. (2022). Radical and ionic meta-C-H functionalization of pyridines, quinolines, and isoquinolines. Science *378*, 779–785. https://doi.org/10.1126/science.ade6029.

32. Kim, M., Koo, Y., and Hong, S. (2022). N-Functionalized Pyridinium Salts: A New Chapter for Site-Selective Pyridine C-H Functionalization via Radical-Based Processes under Visible Light Irradiation. Acc. Chem. Res. *55*, 3043–3056. https://doi.org/10.1021/acs.accounts.2c00530.

33. Schlegel, M., Qian, S., and Nicewicz, D.A. (2022). Aliphatic C–H Functionalization Using Pyridine N-Oxides as H-Atom Abstraction Agents. ACS Catal. *12*, 10499–10505. https://doi.org/10.1021/acscatal.2c02997.

34. Wang, B., Ascenzi Pettenuzzo, C., Singh, J., McCabe, G.E., Clark, L., Young, R., Pu, J., and Deng, Y. (2022). Photoinduced Site-Selective Functionalization of Aliphatic C–H Bonds by Pyridine N-oxide Based HAT Catalysts. ACS Catal. *12*, 10441–10448. https://doi.org/10.1021/acscatal.2c02993.

35. Huo, L., Li, X., Zhao, Y., Li, L., and Chu, L. (2023). Site- and Stereoselective Synthesis of Alkenyl Chlorides by Dual Functionalization of Internal Alkynes via Photoredox/Nickel Catalysis. J. Am. Chem. Soc. *145*, 9876–9885. https://doi.org/10.1021/jacs.3c02748.

36. Lee, W., Park, I., and Hong, S. (2023). Photoinduced difunctionalization with bifunctional reagents containing N-heteroaryl moieties. Sci. China Chem. *66*, 1688–1700. https://doi.org/10.1007/s11426-023-1589-7.

37. Liu, Z., Shi, Z.J., Liu, L., Zhang, M., Zhang, M.C., Guo, H.Y., and Wang, X.C. (2023). Asymmetric C3-Allylation of Pyridines. J. Am. Chem. Soc. *145*, 11789–11797. https://doi.org/10.1021/jacs.3c03056.

38. Nguyen, J.D., D'Amato, E.M., Narayanam, J.M.R., and Stephenson, C.R.J. (2012). Engaging unactivated alkyl, alkenyl and aryl iodides in visible-light-mediated free radical reactions. Nat. Chem. *4*, 854–859. https://doi.org/10.1038/nchem.1452.

39. Arora, A., Teegardin, K.A., and Weaver, J.D. (2015). Reductive Alkylation of 2-Bromoazoles via Photoinduced Electron Transfer: A Versatile Strategy to Csp2–Csp3 Coupled Products. Org. Lett. *17*, 3722–3725. https://doi.org/10.1021/acs.orglett.5b01711.

40. Singh, A., Kubik, J.J., and Weaver, J.D. (2015). Photocatalytic C–F alkylation; facile access to multifluorinated arenes. Chem. Sci. *6*, 7206–7212. https://doi.org/10.1039/c5sc03013g.

41. Arora, A., and Weaver, J.D. (2016). Photocatalytic Generation of 2-Azolyl Radicals: Intermediates for the Azolylation of Arenes and Heteroarenes via C–H Functionalization. Org. Lett. *18*, 3996–3999. https://doi.org/10.1021/acs.orglett.6b01718.

42. Senaweera, S., and Weaver, J.D. (2016). Dual C–F, C–H Functionalization via Photocatalysis: Access to Multifluorinated Biaryls. J. Am. Chem. Soc. *138*, 2520–2523. https://doi.org/10.1021/jacs.5b13450.

43. Singh, A., Fennell, C.J., and Weaver, J.D. (2016). Photocatalyst size controls electron and energy transfer: selectable E/Z isomer synthesis via C–F alkenylation. Chem. Sci. *7*, 6796–6802. https://doi.org/10.1039/c6sc02422j.

44. Boyington, A.J., Riu, M.L.Y., and Jui, N.T. (2017). Anti-Markovnikov Hydroarylation of Unactivated Olefins via Pyridyl Radical Intermediates. J. Am. Chem. Soc. *139*, 6582–6585. https://doi.org/10.1021/jacs.7b03262.

45. Monos, T.M., McAtee, R.C., and Stephenson, C.R.J. (2018). Arylsulfonylacetamides as bifunctional reagents for alkene aminoarylation. Science *361*, 1369–1373. https://doi.org/10.1126/science.aat2117.

46. Seath, C.P., Vogt, D.B., Xu, Z., Boyington, A.J., and Jui, N.T. (2018). Radical Hydroarylation of Functionalized Olefins and Mechanistic Investigation of Photocatalytic Pyridyl Radical Reactions. J. Am. Chem. Soc. *140*, 15525–15534. https://doi.org/10.1021/jacs.8b10238.

47. Seath, C.P., and Jui, N.T. (2019). Intermolecular Reactions of Pyridyl Radicals with Olefins via Photoredox Catalysis. Synlett *30*, 1607–1614. https://doi.org/10.1055/s-0037-1611527.

48. Guan, Y.-Q., Min, X.-T., He, G.-C., Ji, D.-W., Guo, S.-Y., Hu, Y.-C., and Chen, Q.-A. (2021). The serendipitous effect of KF in Ritter reaction: Photo-induced amino-alkylation of alkenes. iScience *24*, 102969. https://doi.org/10.1016/j.isci.2021.102969.

49. Guo, S.-Y., Yang, F., Song, T.-T., Guan, Y.-Q., Min, X.-T., Ji, D.-W., Hu, Y.-C., and Chen, Q.-A. (2021). Photo-induced catalytic halopyridylation of alkenes. Nat. Commun. *12*, 6538. https://doi.org/10.1038/s41467-021-26857-w.

50. Min, X.-T., Ji, D.-W., Guan, Y.-Q., Guo, S.-Y., Hu, Y.-C., Wan, B., and Chen, Q.-A. (2021). Visible Light Induced Bifunctional Rhodium Catalysis for Decarbonylative Coupling of Imides with Alkynes. Angew. Chem. Int. Ed. *60*, 1583–1587. https://doi.org/10.1002/anie.202010782.

51. He, G.-C., Guo, S.-Y., Zheng, H., Liu, C.-H., Li, Y., Min, X.-T., Ji, D.-W., and Chen, Q.-A. (2022). Photo-induced catalytic C—H heteroarylation of group 8 metallocenes. Cell Rep. Phys. Sci. *3*, 100768. https://doi.org/10.1016/j.xcrp.2022.100768.

52. Mei, Y.-K., Min, X.-T., Guo, S.-Y., Liu, C.-H., Zhang, X.-X., Ji, D.-W., Wan, B., and Chen, Q.-A. (2022). Photo-Induced Construction of N-Aryl Amides by Fe Catalysis. Eur. J. Org. Chem. *2022*, e202200043. https://doi.org/10.1002/ejoc.202200043.

53. Yang, F., He, G.-C., Sun, S.-H., Song, T.-T., Min, X.-T., Ji, D.-W., Guo, S.-Y., and Chen, Q.-A. (2022). Selective C-S Bond Constructions Using Inorganic Sulfurs via Photoinduced Electron Donor-Acceptor Activation. J. Org. Chem. *87*, 14241–14249. https://doi.org/10.1021/acs.joc.2c01750.

54. Kouznetsov, V., Mendez, L., and Gomez, C. (2005). Recent Progress in the Synthesis of Quinolines. Curr. Org. Chem. *9*, 141–161. https://doi.org/10.2174/1385272053369196.

55. Madapa, S., Tusi, Z., and Batra, S. (2008). Advances in the Syntheses of Quinoline and Quinoline-Annulated Ring Systems. Curr. Org. Chem. *12*, 1116–1183. https://doi.org/10.2174/138527208785740300.

56. Barluenga, J., Rodríguez, F., and Fañanás, F.J. (2009). Recent advances in the synthesis of indole and quinoline derivatives through cascade reactions. Chem. Asian J. *4*, 1036–1048. https://doi.org/10.1002/asia.200900018.

57. Ramann, G.A., and Cowen, B.J. (2016). Recent Advances in Metal-Free Quinoline Synthesis. Molecules *21*, 986–1009. https://doi.org/10.3390/molecules21080986.

58. Sharma, R., Kour, P., and Kumar, A. (2018). A review on transition-metal mediated synthesis of quinolines. J. Chem. Sci. *130*, 73–98. https://doi.org/10.1007/s12039-018-1466-8.

59. Harry, N.A., Ujwaldev, S.M., and Anilkumar, G. (2020). Recent advances and prospects in the metal-free synthesis of quinolines. Org. Biomol. Chem. *18*, 9775–9790. https://doi.org/10.1039/d0ob02000a.

60. Li, L.H., Niu, Z.J., and Liang, Y.M. (2020). Organocatalyzed Synthesis of Functionalized Quinolines. Chem. Asian J. *15*, 231–241. https://doi.org/10.1002/asia.201901380.

61. Teja, C., and Khan, F.R.N. (2020). Radical Transformations towards the Synthesis of Quinoline: A Review. Chem. Asian J. *15*, 4153–4167. https://doi.org/10.1002/asia.202001156.

62. Duan, K., Tang, J., and Wu, W. (2023). Recent Advances in the Synthesis of Fused Heterocyclic Compounds and Their Antitumor Activities. Chin. J. Org. Chem. *43*, 826–854. https://doi.org/10.6023/cjoc202211046.

63. Popov, K.K., Campbell, J.L.P., Kysilka, O., Hošek, J., Davies, C.D., Pour, M., and Kočovský, P. (2022). Reductive Amination Revisited: Reduction of Aldimines with Trichlorosilane Catalyzed by Dimethylformamide horizontal line Functional Group Tolerance, Scope, and Limitations. J. Org. Chem. *87*, 920–943. https://doi.org/10.1021/acs.joc.1c01561.

64. Woo, J., Christian, A.H., Burgess, S.A., Jiang, Y., Mansoor, U.F., and Levin, M.D. (2022). Scaffold hopping by net photochemical carbon deletion of azaarenes. Science *376*, 527–532. https://doi.org/10.1126/science.abo4282.

65. Zhang, X., Qi, Z., and Li, X. (2014). Rhodium(III)-catalyzed C-C and C-O coupling of quinoline N-oxides with alkynes: combination of C-H activation with O-atom transfer. Angew. Chem. Int. Ed. *53*, 10794–10798. https://doi.org/10.1002/anie.201406747.

66. Qian, B., Guo, S., Shao, J., Zhu, Q., Yang, L., Xia, C., and Huang, H. (2010). Palladium-catalyzed benzylic addition of 2-methyl azaarenes to N-sulfonyl aldimines via C-H bond activation. J. Am. Chem. Soc. *132*, 3650–3651. https://doi.org/10.1021/ja910104n.

67. Qian, B., Xie, P., Xie, Y., and Huang, H. (2011). Iron-catalyzed direct alkenylation of 2-substituted azaarenes with N-sulfonyl aldimines via C-H bond activation. Org. Lett. *13*, 2580–2583. https://doi.org/10.1021/ol200684b.

68. Korbad, B.L., and Lee, S.H. (2014). Synthesis of N-aryl substituted, five- and six-membered azacycles using aluminum-amide complexes. Chem. Commun. *50*, 8985–8988. https://doi.org/10.1039/c4cc04111a.

69. Bhattacharyya, D., Nandi, S., Adhikari, P., Sarmah, B.K., Konwar, M., and Das, A. (2020). Boric acid catalyzed chemoselective reduction of quinolines. Org. Biomol. Chem. *18*, 1214–1220. https://doi.org/10.1039/c9ob02673h.

70. Xu, Y., Gan, Z., Hu, B., and Song, Q. (2012). Convenient Chlorination of Some Special Aromatic Compounds Using N-Chlorosuccinimide. Synthesis *44*, 1074–1078. https://doi.org/10.1055/s-0031-1289732.